Grazing-incidence periodically poled $LiNbO_3$ optical parametric oscillator

Chi-Sheng Yu and A. H. Kung

Institute of Atomic and Molecular Sciences, Academia Sinica, P.O. Box 23-166, Taipei 106, Taiwan

Received March 22, 1999; revised manuscript received July 27, 1999

The design and operation of a pulsed quasi-phase-matched periodically poled lithium niobate optical parametric oscillator in the grazing incidence configuration are described. A narrow bandwidth of 0.3 cm^{-1} is demonstrated over most of the full tuning range of the device. Broad and rapid scanning has been achieved by rotation of a single mirror. Long-term stable operation and a pump-to-signal power efficiency of 46% are shown to be possible. Methods to improve the bandwidth are discussed. © 1999 Optical Society of America [S0740-3224(99)03211-7]

OCIS codes: 140.3600, 140.3070, 190.2620, 190.4410, 190.4970, 230.4720.

1. INTRODUCTION

Recent advances in engineered nonlinear optical materials have renewed interest in the development of optical parametric oscillators (OPO's) as compact, broadly tunable solid-state coherent sources of radiation.[1] By use of the technique of quasi-phase matching (QPM) to compensate for phase-velocity mismatch in parametric interactions, several efficient frequency-conversion devices have been demonstrated.[2] QPM offers many significant benefits. It permits the selection of a large nonlinear coefficient of interaction. Noncritical phase matching can be achieved for any wavelength within the material's transparency range. Tuning can conveniently be done with temperature, the grating period engineered into the material, and angle. Several materials, e.g., $LiNbO_3$,[2] $KTiOPO_4$,[3] $RbTiAsO_4$,[4] and $LiTaO_3$ (Ref. 5), are being developed for QPM. However, periodically poled $LiNbO_3$ (PPLN) is the most advanced of these and has become commercially available. Lithographic masking and planar processing used in the microelectronic industry are applied to manufacture quasi-phase-matched PPLN wafers. Optical polishing and antireflection coating developed for bulk material can be extended to the processing of these wafers. Thus the material can be supplied in a large quantity and at a relatively affordable price. Aligning the electric field of all the interacting waves parallel to the z axis of PPLN yields an enhancement in the strength of nonlinear parametric interactions that is approximately 20 times greater than that of the conventional phase-matched arrangement.

Two highly desirable properties of the OPO are its broad tunability and its simplicity of use for rapid scanning. For many applications, a narrow bandwidth is important. There are several techniques to produce a narrow bandwidth. The use of intracavity line-narrowing elements such as gratings and etalons[6,7] or injection seeding of the OPO cavity with a narrow-band laser[8,9] have proved to reduce the OPO's bandwidth considerably. Indeed, cw single-longitudinal-mode OPO's have already been demonstrated and used, for instance, in trace-gas detection applications.[10] However, the use of these techniques must compromise the tuning range and the scanability of the OPO's, owing to the spectral coverage of each seeder and etalon elements. Another approach to producing narrow bandwidths is to configure the OPO cavity with a grazing-incidence–grating-mirror combination.[11,12] This approach has had good success with tunable lasers and visible OPO's. Extremely narrow-bandwidth (single-longitudinal-mode or nearly single-longitudinal-mode) operation has been achieved in $KTiOPO_4$ and β-BaB_2O_4 OPO's.[13,14] Yet grazing-incidence OPO's have not been reported for the infrared. The main reason for this is that the grazing-incidence configuration suffers intrinsically higher loss compared with the conventional cavity configuration. Hence a high gain medium or high gain interaction is necessary to counter this shortcoming. Infrared materials with large nonlinear coefficients have a low optical damage thresholds,[15] so that has not been realistic to use the grazing-incidence approach in the infrared. Recent advancements in PPLN material have made this approach feasible.

We have designed a grazing-incidence OPO based on QPM PPLN pumped by a diode-pumped Nd:YAG laser. Our goal is to obtain high power in the infrared with high efficiency, broad tuning, and narrow bandwidth in a compact all-solid-state device. In this paper we report on the performance of this OPO and discuss its possibilities and limitations.

2. EXPERIMENTAL SETUP

A schematic diagram of the grazing-incidence OPO is shown in Fig. 1. The OPO is configured for single resonance at the signal wavelength. Input mirror M1 is highly transmitting ($T > 90\%$) at 1064 nm and highly reflecting ($R > 99\%$) at the signal wavelength. Owing to the broad operating range of the PPLN crystals, two mirrors are used as M1. One of the mirrors is coated for high reflection from 1.6 to ~2.0 μm; the second mirror, from 1.4 to 1.7 μm. The rear mirror is silver coated, with

a surface quality of λ/10. The grating is a standard 26-mm-wide replica grating blazed at 1.85 μm with a 600/mm groove density. It is silver coated with a MgF_2 overcoat. The grating is placed at grazing incidence relative to the cavity axis. The angle of incidence α varies from 84.5° to 89.3°. The grooves of the grating are such that reflections of the OPO signal wave are in the *s* plane of the grating. The first-order reflection from the grating is reflected back into the cavity from rear mirror M2. The zeroth-order reflection of the grating acts as the output coupling of the OPO cavity.

The PPLN crystal is installed in a temperature-controlled oven that is supported on an $X-Y$ translator. The crystal temperature is held to within 0.1 °C. Two crystals are used. Each crystal is 11 mm wide, 0.5 mm thick, and 50 mm long, with the *z* axis of the crystal oriented normally to the largest plane of the crystal. There are eight separate grating periods poled onto the crystal. Each period is 1.3 mm wide and 50 mm long. The values of the periods are predetermined by the crystal supplier, Crystal Technology, Inc. The period values and the wavelength range that they cover are listed in Table 1. The end faces of the crystal are polished and coated for antireflection (<0.5%/surface) from 1.4 to 2.0 μm. The reflection loss at the pump wavelength was measured to be 5%/surface. The longitudinal axis of the crystal is tilted relative to the cavity axis to minimize the amount of broad-bandwidth parametric generation initiated by feedback from the crystal surfaces. We achieve coarse tuning of the OPO by setting the temperature of the crystal and choosing the crystal grating period. Fine scanning is achieved by rotation of the rear mirror with a microstepping motor attached to a micrometer. The cavity length is 16 cm, which yields a cavity mode spacing of 0.94 GHz.

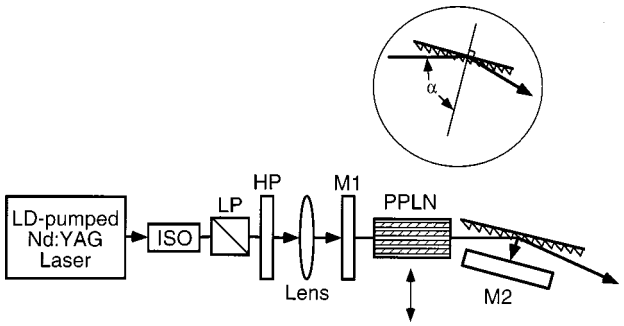

Fig. 1. Schematic of the OPO: ISO, optical isolator; LP, linear polarizer; HP, half-wave plate. Inset, angle of incidence α.

Table 1. Descriptions of PPLN Crystals Used

Crystal Identification	Grating Period (μm)	Signal Wavelength (μm)	Idler Wavelength (μm)
97-02182-07	28.5	1.458–1.486	3.743–3.936
	28.7	1.468–1.499	3.664–3.864
	28.9	1.479–1.514	3.578–3.788
	29.1	1.491–1.530	3.490–3.710
	29.3	1.505–1.549	3.398–3.630
	29.5	1.519–1.569	3.302–3.548
	29.7	1.535–1.594	3.200–3.463
	29.9	1.554–1.622	3.090–3.374
97-02256-02	30.0	1.564–1.639	3.032–3.328
	30.2	1.585–1.677	2.908–3.234
	30.4	1.611–1.729	2.766–3.133
	30.6	1.642–1.807	2.586–3.020
	30.8	1.679–1.956	2.332–2.902
	30.95	1.714–2.128	2.128–2.804
	31.1	1.758–2.128	2.128–2.695
	31.2	1.785–2.128	2.128–2.613

The pump laser is a commercial laser-diode-pumped acousto-optic *Q*-switched Nd:YAG laser (Lightwave Electronics Model 210S). For most measurements the laser was operated at 3 kHz with a pulse duration of 28 ns and a maximum pulse energy of 0.8 mJ. The laser is focused to a Gaussian waist radius ($1/e^2$) of 220 μm, and the waist position is located at the center of the PPLN crystal. The bandwidth of the laser is 0.6 cm^{-1} according to the laser's specifications.

Bandwidth measurements are performed with a McPherson, Inc., Model 2035 0.35-m Czerny–Turner scanning monochromator fitted with a CCD camera detector. The wavelength and the resolution of the monochromator are calibrated with a He–Ne laser that has a maximum bandwidth of 1090 MHz. Inasmuch as the CCD camera is sensitive only to visible and near-infrared light, the bandwidth of the non-phase-matched second harmonic of the OPO signal radiation that is concurrently generated by the PPLN crystal is measured. The bandwidth of the OPO signal wavelength, which is $1/\sqrt{2}$ of the bandwidth of the second harmonic, can then be determined. We establish the statistical error and the experimental uncertainty of the bandwidth by repeating a bandwidth measurement ten times. The power of the second-harmonic output is not measurable by the powermeter; however it is sufficiently intense to cause near saturation of the sensitive CCD camera. Output power is determined with a thermopile (Molectron Corporation). We measure the OPO efficiency by monitoring the depletion of the pump laser pulse with a fast photodiode and a 1-GHz digital sampling oscilloscope (LeCroy Model LC433A).

As a demonstration of the application of the OPO, we take sample absorption spectra by monitoring the photoacoustic signal generated in a cell filled with 16 Torr of methane gas while the OPO output wavelength is scanned. Because methane has absorption lines in both the 1.64- and the 3.3-μm regions, the bandwidths of both the signal and the idler outputs of the OPO can also be examined after calibration of the absorption spectra.

3. RESULTS

The main focus of this study is on the bandwidth characteristics of the grazing-incidence OPO. After the bandwidth characteristics were established, we measured the efficiency of the OPO at the largest feasible angle of incidence by measuring the depletion of the pump radiation. Finally, we used the OPO to obtain photoacoustic absorption spectra of methane.

Unless otherwise stated, the results reported here were obtained at an oven temperature of 190 °C, with a crystal

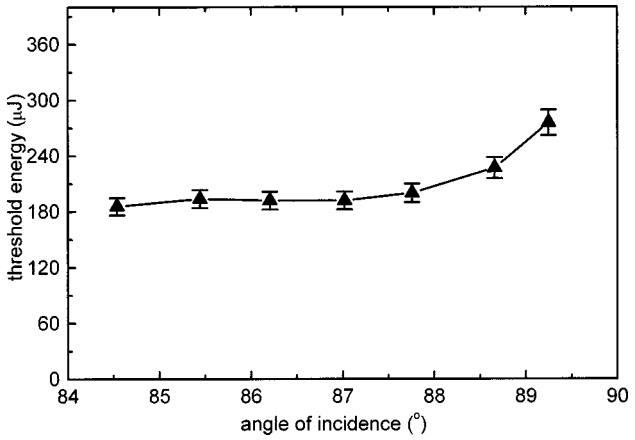

Fig. 2. OPO threshold as a function of the angle of incidence.

grating period of 29.5 μm, or both. The results were found to be representative of the OPO characteristics at other temperature and crystal period values as long as the signal wavelength was >10% from degeneracy. Performance close to degeneracy was not studied because a suitable coating for the input mirror was not available.

To establish a benchmark for all the measurements we first substituted a 50% output coupler for the grating–rear mirror pair to set up a conventional OPO cavity. The threshold for this cavity arrangement was determined to be 90 μJ, and the bandwidth was roughly 3 cm^{-1}. At the full pump power, the signal pulse energy was 250 μJ for a net pump-to-signal power conversion of 25% and a photon conversion of 41%.

We made the first measurements with the grating in place to determine the OPO characteristics as a function of the angle of incidence, α. When α was changed from 84.5° to 89.3°, the OPO threshold increased from 185 to 275 μJ, as shown in Fig. 2, in line with losses that are due to the zeroth-order grating reflection (equivalent output coupling), which increased from 42% at $\alpha = 84.5°$ to >80% at $\alpha = 89.3°$. The threshold at 84.5° was already substantially higher than that of the benchmark cavity because the grating efficiency into the first order is only 80%. Yet there is instant improvement in the bandwidth on insertion of the grating into the cavity at $\alpha = 84.5°$. The bandwidth gradually reduces to the best value of 0.3 cm^{-1}, with α increased to 89.3° (Fig. 3). At this angle, the projection of the axial beam on the grating was wider than 26 mm, and a portion of this beam was clipped by the edge of the grating and exited the cavity in the direction of the cavity axis. The bandwidth of this portion of the beam was found to be similar to that of the main output beam.

A major attraction of the OPO is its broad tuning range. Hence it is important to study the bandwidth as the OPO is tuned. There are several ways to tune this OPO. One achieves coarse tuning of the output wavelength by changing the crystal temperature, the crystal grating period, or both. Figure 4 shows the bandwidth of the peak signal wave as a function of the temperature of the crystal. Incidence angle α was fixed at 89.3°. At each temperature we had to adjust the rear mirror to search for the peak wavelength. Figure 5 shows the OPO bandwidth at 190 °C when the crystal grating period was altered by translation of the crystal in the direction shown in Fig. 1. Each data point represents the peak wavelength output for the corresponding grating period. Two crystals were used to cover the wavelength range shown. Clearly these results show that the bandwidth is

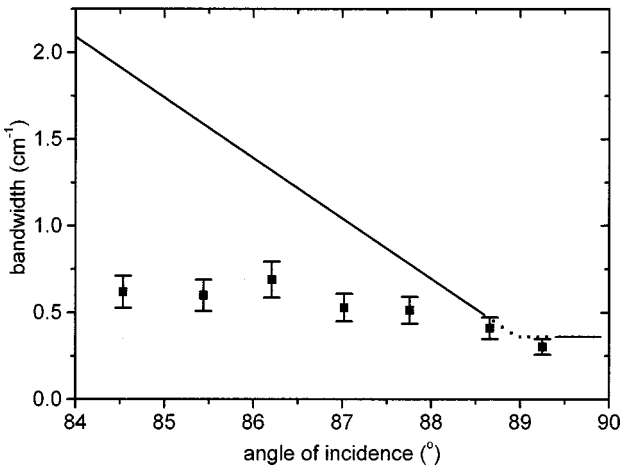

Fig. 3. OPO signal bandwidth versus angle of incidence. The solid curve was calculated from Eqs. (1) and (3). The dotted curve implies the theoretical transition from Eq. (1) to Eq. (3) at the angle α given by relation (2).

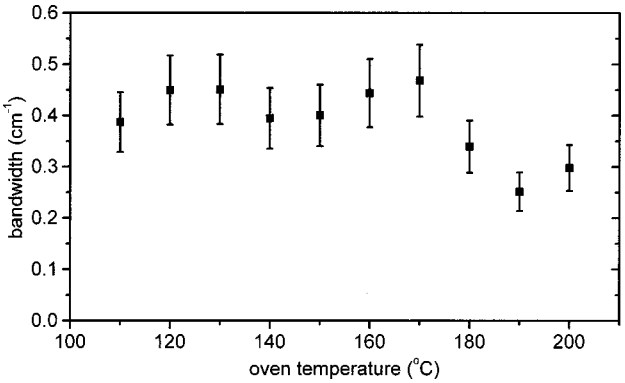

Fig. 4. Measured OPO signal bandwidth for various oven temperatures. The PPLN crystal temperature cannot be measured directly.

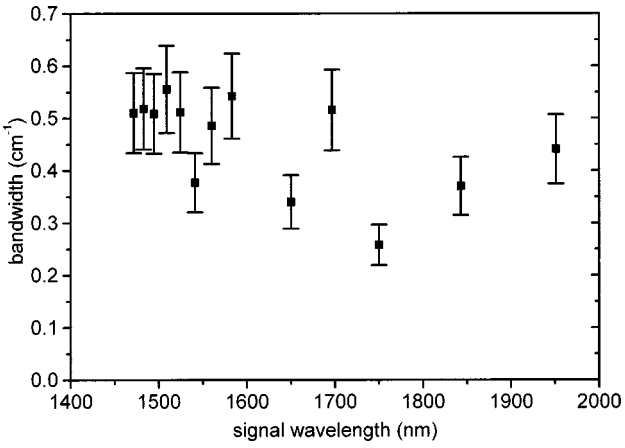

Fig. 5. Measured OPO signal bandwidth for several PPLN crystal grating periods. Each point represents the peak wavelength for the corresponding grating period.

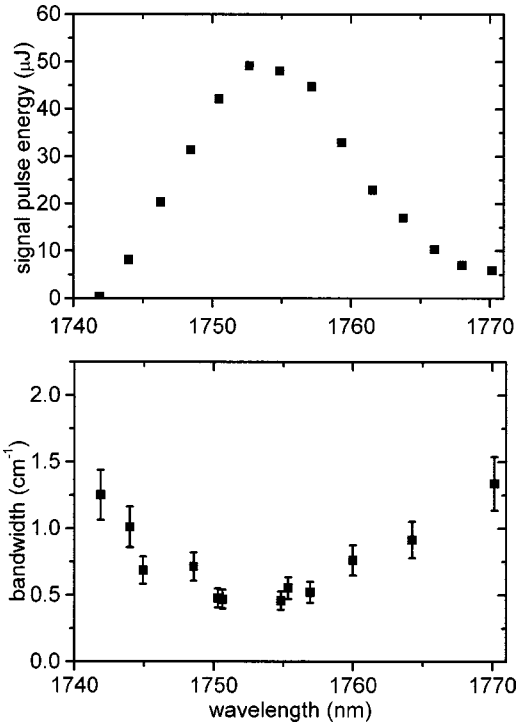

Fig. 6. Top, the signal pulse energy and bottom, the corresponding bandwidth versus output wavelength changed by the fine tuning of the position of the rear mirror. A broadband background energy of 13 μJ has been subtracted from the values shown.

not strongly affected by changes in the crystal's temperature or the crystal's period over essentially the entire tuning range of the PPLN OPO. They point to the unsurprising evidence that the grating is the determining factor for the bandwidth of the grazing-incidence OPO. The variations in bandwidth with temperature in Fig. 4 were within the statistical error bar of each data point and can be considered incidental, although the bandwidths appear to favor a higher temperature. The bandwidth varies with crystal period over a wider range than with temperature. We observed that the threshold of the OPO is lower for the crystal periods that show a smaller bandwidth. This result indicates that the larger variation in bandwidth could be due to a nonuniform quality in the fabrication of the period and to the quality of the crystal substrate itself.

The use of an intracavity grating affords continuous and fine tuning of the OPO output wavelength. Figure 6 displays the output pulse's energy and bandwidth as a function of the output wavelength. Tuning was achieved by rotation of the rear mirror. The figure shows that one can obtain a broad tuning range by simply rotating the rear mirror. The FWHM range shown is 45 cm^{-1}. Significantly, this range is equal to nearly twice the acceptance bandwidth of the crystal period used. This phenomenon holds true for all the poled periods studied. As one can see from the figure, the output bandwidth remains fairly constant within the half-width of the tuned range but increases rapidly if the OPO is tuned outside the half-power range. There was ~13 μJ of parametrically generated broadband output when the grating was blocked. It is our conjecture that the increase in bandwidth is a consequence of the dynamics of competition between the power buildup in the grating oscillator and the broadband parametric generation.

To demonstrate the utility of this OPO in spectroscopic applications, we obtained an overtone spectrum of methane as shown in Fig. 7, photoacoustic detection of the absorption by methane at the signal wavelength. This spectrum has been normalized to the output power of the OPO. The line intensities are a convolution of the absorption strength, the OPO bandwidth, and the density of methane lines within the OPO bandwidth. Because the methane line positions are well known and the Doppler linewidth of methane is small compared with the resolution of the spectrum, one can use the spectrum to determine the OPO bandwidth. Table 2 lists the peak positions of the lines and their widths. The peak positions were obtained from calibrated spectroscopic data.[16] We used them to calibrate this spectrum, which in turn we used to determine the linewidths. It can be seen that the width of the two most intense peaks (numbered 2 and 3) is 0.3 cm^{-1}, in good agreement with measurements obtained with the monochromator. Peaks 1 and 4 of the spectrum fall outside the FWHM range of the OPO output power, and they are wider, also in agreement with the trend that is shown in Fig. 6.

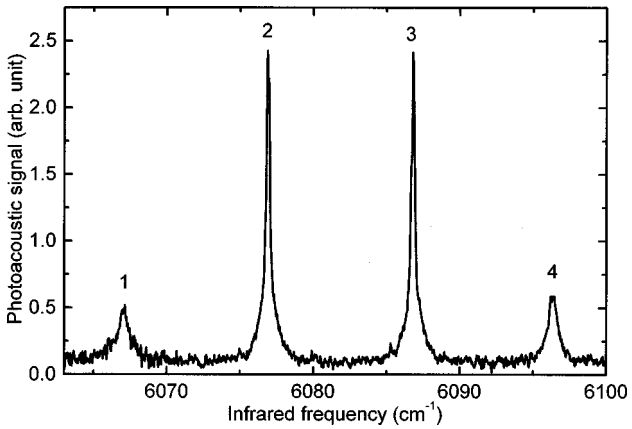

Fig. 7. Optoacoustic spectrum of methane in the vicinity of 6080 cm^{-1} (1.64 μm). The numbers 1–4 identify the peak positions given in Table 2.

Table 2. Assignment of Peak Positions Shown in Figs. 7 and 8 and Measured Widths of the Corresponding Lines

Peak Number[a]	Peak Position (cm^{-1})	Linewidth (cm^{-1})
1*	6067.0	0.7
2	6077.0	0.3
3	6087.0	0.3
4*	6096.3	0.7
5	3028.75	0.85
6	3038.55	0.9
7	3048.05	0.9
8	3057.80	1.0
9*	3067.25	1.0
10*	3076.60	1.2

[a] Peaks marked* are outside the FWHM power of the tuned range.

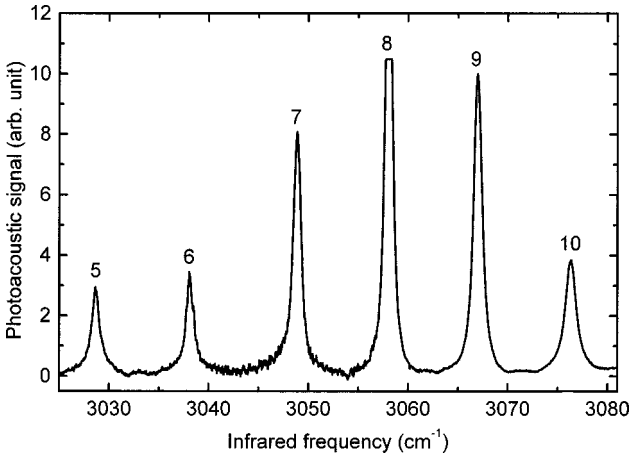

Fig. 8. Optoacoustic spectrum of methane in the vicinity of 3050 cm^{-1} (3.28 μm). A Ge filter was inserted in front of the cell window to transmit the idler frequency only into the cell when this spectrum was taken. The numbers 5–9 identify the peak positions given in Table 2.

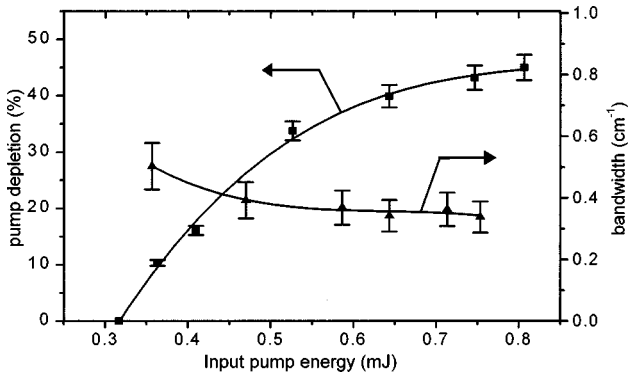

Fig. 9. Measured pump depletion (■) and output bandwidth (▲) as the input pump pulse energy is varied from threshold to the maximum available value. The curves drawn through the data points are polynomial fitted curves used only for the purpose of guiding the eye.

The C—H fundamental stretching vibration of methane is near 3.3 μm. It can be probed by the idler output of the OPO, which is collinear with the signal output. Such a spectrum is shown in Fig. 8. The spectrum shows that the scan range achieved was more than 55 cm^{-1}. The peak positions and their widths are also listed in Table 2. The linewidths in the spectrum are typically 0.9 cm^{-1}. Peak 8 is wider because it was saturated. These widths represent the bandwidths of the idler wavelength and are slightly wider than the theoretical convoluted width of the signal bandwidth (0.3–0.4 cm^{-1}) and the pump laser bandwidth (0.6 cm^{-1}).

Grazing-incidence OPO's reported in the literature operate with an efficiency of a few percent.[13,14] This is so because they were operated primarily near threshold when the pump intensity was already close to the damage limit of the gain material. Use of quasi-phase matching, however, raised the parametric gain substantially and thus lowered the threshold for oscillation while the damage limit was unchanged. The OPO that we configured has been operated at 2.5 times above threshold for hundreds of hours without incurring visible damage. We measured the PPLN OPO efficiency as a percent of pump depletion by comparing the energy of the pump pulse transmitted through the cavity with and without the rear mirror in alignment. The results are plotted in Fig. 9, which shows the percent pump depleted as a function of input energy. It reaches a value close to saturation at a pump level that is 2.5 times above threshold. The bandwidth remains fairly constant, except when it is close to threshold, where it is slightly higher. These efficiencies are believed to be the highest efficiencies reported for grazing-incidence configured OPO's.

4. DISCUSSION

The primary factor that lies behind the idea of a grazing-incidence configuration is to fill the grooves of a grating to make use of the grating's maximum resolving power by tilting to the maximum the angle of the grating relative to the cavity axis. The single-pass resolution $\Delta\nu_d$ obtainable is limited by the diffraction of the incident beam and is given by the formula[11]

$$\Delta\nu_d = \frac{1}{\pi\omega_g \tan\alpha}, \tag{1}$$

where α is the incidence angle of the OPO beam and ω_g is the Gaussian beam waist, and $\Delta\nu_d$ is in inverse centimeters. From Eq. (1), it is clear that one would want to use a large beam size and a large incidence angle to obtain a narrow bandwidth. Equation (1) is valid until the diffracting beam fills width d of the grating. For a Gaussian beam, and in the optimal case in which the center of the grating is located at one Rayleigh length $L_R = \pi\omega^2/\lambda$ away from the cavity waist, the validity condition is

$$2\sqrt{2}\omega_g \tan\alpha \leqslant d \sin\alpha, \tag{2}$$

beyond which Eq. (1) becomes

$$\Delta\nu_{d,\min} = \frac{2\sqrt{2}}{\pi d \sin\alpha}, \tag{3}$$

which is the well-known bandwidth expression for grazing-incidence cavities with the first-order diffracted beam angle equal to 0°.[17]

As the OPO signal wave is building up, the signal wave travels through the grating filter a multiple number of times, and further filtering is possible. For a Gaussian pass function, the bandwidth can be narrowed additionally by the square root of the number of passes N.[6] The final bandwidth is then given by

$$\Delta\nu_{\mathrm{OPO}} = \frac{1}{\sqrt{N}} \times \Delta\nu_d\,. \tag{4}$$

The solid curve in Fig. 3 is the net bandwidth in a single pass as determined by Eq. (1) and relation (3) as a function of α for this OPO. The break in the curve shows where the equality in relation (2) is reached. The curve shows that a bandwidth of 0.36 cm^{-1} could be achieved in a single pass in the grazing-incidence configuration. The measured values are generally below the curve, reflecting the contribution from multiple round-trip passes through

the cavity. This contribution is quite significant at small values of α, but when $\alpha \geqslant 89°$, where the cavity lifetime approaches one round trip, its effect clearly is offset by other factors such as saturation broadening.

The bandwidth of several tenths of an inverse centimeter is respectable, but is far from being single longitudinal mode (SLM), which is most desirable. It is easy to see from Eq. (3) that improvements to the bandwidth can be obtained by use of a wider grating, which will reduce the limiting resolution to less than 0.1 cm^{-1} (10-cm-wide grating). If SLM operation is desired, the cavity mode spacing must be increased to approximately 1.5 GHz. This value corresponds to a cavity length of 10 cm, which, with the grating width and a 5-cm-long crystal, means that some ingenious cavity component arrangement must be devised. The use of a SLM pump laser will be necessary to sustain SLM operation.[14,18]

For the grazing-incidence configuration to be useful, it is important that the bandwidth stay uniform as the OPO is tuned. The present device has not performed to this standard. As is shown in Fig. 6, this OPO's bandwidth broadens when the OPO is tuned off its peak wavelength where the gain becomes smaller. There is a small amount of signal and idler feedback from the exit facet of the crystal. Inasmuch as the single-pass gain is high, this feedback was sufficient to cause broadband generation between mirror M1 and the crystal facet and negatively affects the output bandwidth. We attempted to reduce the amount of this feedback by tilting the crystal facet relative to the pump beam's direction. To further reduce or eliminate this feedback one could fabricate the crystal with a wedge between the input and output facets of the crystal.[10] We estimate that for the dimensions of the present crystal, a 1°–2° wedge would be sufficient to produce the desired effect.

Finally, it is useful to discuss the feasibility of rapid scanning. The spectrum shown in Fig. 7 consists of 1750 data points, the number needed to maintain the spectral resolution as the wavelength was scanned. Operating the laser at a repetition rate of several kilohertz and acquiring data at ~1 kHz will complete this spectrum in just several seconds. Hence it is entirely feasible to build an all-solid-state OPO-based device for use as a portable rapid-scan infrared spectrometer for gas monitoring and mobile remote-sensing applications.

ACKNOWLEDGMENTS

We thank Joachim Knittel and Jr-i Lee for their contributions to the initial phase of this study.

A. H. Kung's e-mail address is akung@po.iams.sinica.edu.tw.

REFERENCES

1. L. E. Myers, R. C. Eckhardt, M. M. Fejer, R. L. Byer, W. R. Bosenberg, and J. R. Pierce, "Quasi-phase-matched optical parametric oscillators in bulk periodically poled $LiNbO_3$," J. Opt. Soc. Am. B **12**, 2102–2116 (1995).
2. L. E. Myers and W. R. Bosenberg, "Periodically poled lithium niobate and quasi-phase-matched optical parametric oscillators," IEEE J. Quantum Electron. **33**, 1663–1672 (1997), and references therein.
3. Q. Chen and W. P. Risk, "Periodic poling of $KTiOPO_4$ using an applied electric field," Electron. Lett. **30**, 1516–1517 (1994).
4. H. Karlsson, F. Laurell, P. Henriksson, and G. Arvidsson, "Frequency doubling in periodically poled $RbTiOAsO_4$," Electron. Lett. **32**, 556–557 (1996).
5. K. Mizuuchi, K. Yamamoto, and M. Kato, "Generation of ultraviolet light by frequency doubling of a red laser diode in a first order periodically poled bulk $LiTaO_3$," Appl. Phys. Lett. **70**, 1201–1203 (1997).
6. S. J. Brosnan and R. L. Byer, "Optical parametric oscillator threshold and linewidth studies," IEEE J. Quantum Electron. **15**, 415–431 (1979).
7. T. K. Minton, S. A. Reid, H. L. Kim, and J. D. McDonald, "A scanning single-mode $LiNbO_3$ optical parametric oscillator," Opt. Commun. **69**, 289–293 (1989).
8. M. J. T. Minton, T. D. Gardner, G. Chourdakis, and P. T. Woods, "Injection seeding of an infrared optical parametric oscillator with a tunable diode laser," Opt. Lett. **19**, 281–283 (1994).
9. G. W. Baxter, H. D. Barth, and B. J. Orr, "Laser spectroscopy with a pulsed, narrowband infrared optical parametric oscillator system: a practical, modular approach," Appl. Phys. B: Lasers Opt. **66**, 653–657 (1998).
10. P. E. Powers, T. J. Kulp, and S. E. Bisson, "Continuous tuning of a cw periodically poled lithium niobate optical parametric oscillator by use of a fan-out grating design," Opt. Lett. **23**, 159–161 (1998).
11. I. Shoshan, N. N. Danon, and U. P. Oppenheim, "Narrowband operation of a pulsed dye laser without intracavity beam expansion," J. Appl. Phys. **48**, 4495–4497 (1977).
12. M. G. Littman and H. J. Metcalf, "Spectrally narrow pulsed dye laser without a beam expander," Appl. Opt. **17**, 2224–2227 (1978).
13. W. R. Bosenberg and D. R. Guyer, "Broadly tunable, single-frequency optical parametric frequency-conversion system," J. Opt. Soc. Am. B **10**, 1716–1722 (1993).
14. L. A. W. Gloster, I. T. McKinnie, Z. X. Jiang, T. A. King, J. M. Boon-Engering, W. E. van der Veer, and W. Hogervorst, "Narrow-band β-barium borate optical parametric oscillator in a grazing-incidence configuration," J. Opt. Soc. Am. B **12**, 2117–2121 (1995).
15. See, for example, V. G. Dmitriev, G. G. Gurzadyan, and D. N. Nikogosyan, "Properties of nonlinear optical crystals," in *Handbook of Nonlinear Optical Crystals*, 2nd ed., A. E. Siegman, ed. (Springer, New York, 1997), Vol. 64.
16. "The National Institute of Standards and Technology (NIST) chemistry webbook," http://webbook.nist.gov/chemistry.
17. M. G. Littman, "Single-mode operation of a grazing-incidence pulsed dye laser," Opt. Lett. **3**, 138–140 (1978).
18. J. M. Boon-Engering, W. E. van der Veer, E. A. J. M. Bente, and W. Hogervorst, "Scanning and locking of a single longitudinal mode β-barium borate OPO in a grazing incidence configuration," Opt. Commun. **136**, 261–266 (1997).